THE AMERICAN SOCIETY OF MECHANICAL ENGINEERS
345 E. 47th St., New York, N.Y. 10017

98-GT-581

COMBUSTION OSCILLATION ANALYSIS OF PREMIXED FLAMES AT ELEVATED PRESSURES

MASAYA OHTSUKA
SHOHEI YOSHIDA
SHIN'ICHI INAGE
NARIYOSHI KOBAYASHI
Power & Industrial Systems R&D Division, Hitachi Ltd.
832-2 Horiguchi, Hitachinaka-shi, Ibaraki-ken, 312 Japan

ABSTRACT

A new analytical time lag flame model based on Bloxidge's flame model was introduced for calculating combustion oscillation of premixed flame to take into account the distribution of heat release rate and flame speed which was calculated by analytical formulas dependent on pressure, temperature, fuel-to-air ratio and velocity. The transfer matrix technique using the new flame model was applied to the calculation of acoustic resonance. To verify the model, combustion oscillation experiments were performed for methane-air premixed flames stabilized by a swirl burner at elevated pressures between 0.6 - 0.9MPa. Fluctuating pressure had the maximum peak at the specific value of $f\tau_f$. Here f is the frequency of resonance and τ_f is the passing time of premixed gas through flame length. The analysis could simulate the dependency of fuel-to-air ratio and static pressure for dynamic pressure local peak.

NOMENCLATURE

A_{O2}	Mass Fraction of O_2 in Air (-)
a	Speed of Sound (m/s)
C_p	Specific Heat Capacity (J/kgK)
E_0	Activation Energy (K)
F/A	Fuel-to-Air Ratio (-)
f	Frequency(Hz)
G	Acoustic Amplification Factor (-)
G_f	Flame Response Function (-)
k	Wave Number (1/m)
L_f	Total Flame Length (m)
L_m	Flame Length until Heat Maximum (m)
l	Flow Path Length (m)
l_t	Taylor Microscale(m)
M_{O2}	Molecular Weight of O_2 (kg/kmol)
P	Static Pressure (ata)
p	Fluctuating Pressure (ata)
Q	Mean Heat Release Rate per Unit Length (W/m^4)
q	Fluctuating Heat Release Rate per Unit Length (W/m^4)
R_t	Turbulent Reynolds Number (-)
r_B	Center Rod Radius of Burner (m)
r_o	Air Path Outer Radius of Burner (m)
S	Flow Path Cross Section Area (m^2)
S_t	Turbulent Flame Speed (m/s)
S_u	Laminar Flame Speed (m/s)
T	Absolute Temperature (K)
U_f	Axial Velocity at Flame (m/s)
U_u	Axial Velocity at the Outlet of the Burner (m/s)
u	Fluctuating Velocity (m/s)
v_t	Turbulent Velocity(m/s)
W	Acoustic Energy (J/m^2)
x	Axial Length (m)
Y	Fuel Mass Fraction (-)
α	Frequency Factor (mol/m^{3}s)
Γ	Attenuation Factor
ΔW	Oscillation Energy (J/m^2)
η	Mass Flow Rate Fluctuation (kg/s)
ϑ	Flame Angle (rad)
λ	Heat Conduction Rate (W/mK)
ν	laminar kinematic viscosity(m^2/s)
τ_f	Lag Time through Flame(s)

Presented at the International Gas Turbine & Aeroengine Congress & Exhibition
Stockholm, Sweden — June 2–June 5, 1998

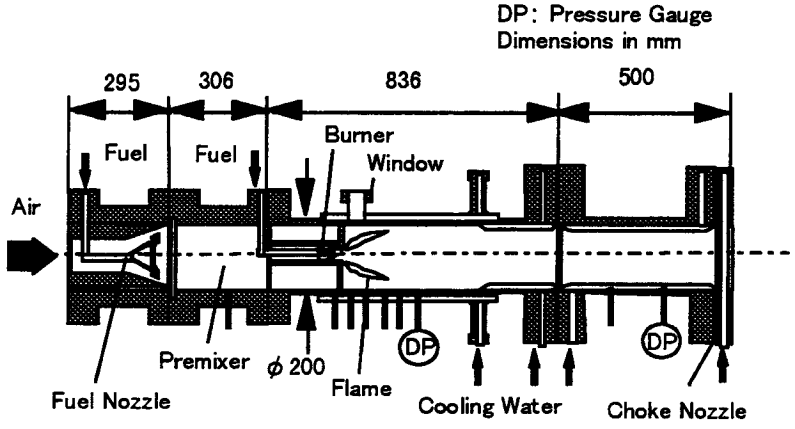

Figure 1. Test Facility

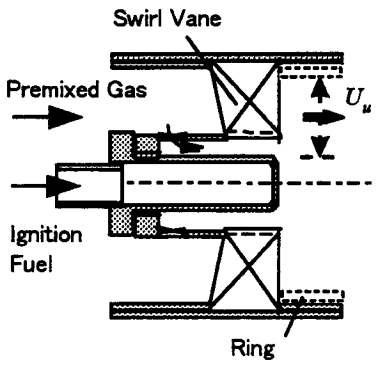

Figure 2. Test Burner

τ_m	Lag Time until Heat Maximum(s)
χ	Heat Release Parameter = $(T_b-T_u)/T_u$
ω	Angular Velocity (rad/s)
i	Flow Path Number
b	Burned Side of Flame
u	Unburned Side of Flame
I	Imaginary Part
R	Real Part

INTRODUCTION

The reduction of combustion oscillation is one of the most important tasks for the development of low NOx combustors because combustion oscillation tends to occur with the reduction of NOx and it may cause irreparable damage to combustors. Premixed flame has been widely used to reduce NOx, but combustion oscillation is induced due to the flame instability. The oscillation can be self-excited oscillation generated by the feedback loop of acoustic systems including flames. Combustion oscillation occurs when the Rayleigh's criterion is satisfied, that is, fluctuating pressure and fluctuating heat release rate are in phase for a period of oscillation. The condition is achieved by the phase matching of the acoustic time, which is set by the combustor length, and the combustion time, which is characterized by the burning time of premixed gas. There are many analytical models of combustion oscillation, which were introduced by review papers (for example, S. Candel(1996), R. J. Raun et al.(1993)). But the onset of combustion oscillation has not been well predicted because the phenomenon is affected by many factors such as pressure, temperature, fuel-to-air ratio, velocity, geometrical configuration and so on. It is very important to clarify the dependency of these factors for combustion oscillation when investigating the phenomenon and designing combustors. The objectives of this study are to elucidate the relationship of these factors and to develop a new analytical model for combustion oscillation.

The transfer matrix approach is useful to calculate the acoustic mode in a one-dimensional network system. Bohn and Deuker(1993) calculated the stability of combustion oscillation by evaluating an acoustic amplifying factor calculated by using a transfer matrix. The analysis results were crucially dependent on the transfer matrix of the flame, but so far the flame model has not been well established. Rayleigh's criterion shows that combustion oscillation is strongly coupled with fluctuating heat release rate. Bloxidge et al.(1988) studied premixed flame in a duct and introduced an experimental formulation of fluctuating heat release rate in relation to inlet velocity fluctuation.

In this study, a new flame model for transfer matrix analysis was introduced by using Bloxidge's model, assuming the distribution of mean heat release rate and a turbulent flame speed model for evaluating flame length. The authors' HTA (Hyperbolic Tangent Approximation) model was applied to the calculation of turbulent flame speed which is dependent on pressure, temperature, fuel-to-air ratio and velocity. To verify the model, combustion oscillation experiments were performed for methane-air premixed flames stabilized by a swirl burner with elevated pressures.

TEST FACILITY

Figs.1 and 2 show test facility and test burner. The test section was a straight pipe of 200mm inner diameter and the premixed burner was located at the center of the pipe. A choke nozzle was set at the outlet of the test section to clarify the outlet acoustic boundary condition. An inlet pipe of 66mm inner diameter and 151mm length, which was attached to the burner, was connected to the premixer (200mm inner diameter). The area difference between the premixer and the inlet pipe made the acoustic boundary condition nearly open. Fuel methane was injected and mixed with air within ~2% of the mean standard deviation of fuel concentration distribution at the inlet of the burner. The burner

was a swirl burner which had an ignition fuel nozzle at the center and 30° swirl vanes surrounding the fuel nozzle.

The experimental conditions were as follows:

Pressure	0.51 - 1.48 MPa
Inlet Temperature	235 - 395 ℃
Fuel Air Ratio	0.03 - 0.045
Flow Rate	0.27 - 0.52 kg/s
Burner Outlet Velocity	30 - 45m/s

In this paper, pressure was 0.6 - 0.9MPa, temperature was 370-395 ℃ mainly. Burner outlet velocity could be changed by inserting a ring at the outlet of the burner but it was fixed ~40m/s with a ring of 53mm inner diameter.

ANALYSIS METHOD

In this study, physical properties were assumed to be constant in the lateral direction and assumed to change only in the axial direction. Stability of the acoustic wave was evaluated by linear analysis. The stability of combustion oscillation was calculated by Bohn and Deuker's method using an acoustic amplifying factor. The relationship of pressure fluctuation p and mass flow rate fluctuation η at two points were formulated by transfer matrices. An acoustic wave was divided into two traveling waves which proceeded in positive(+) and negative(−) directions. The acoustic amplifying factor G for an acoustic system was calculated as follows:

$$G = G_f^+ G_u G_f^- G_b \tag{1}$$

$$G_f^+ = \frac{\eta_b^+}{\eta_u^+},\quad G_u = \frac{\eta_u^+}{\eta_u^-},\quad G_f^- = \frac{\eta_u^-}{\eta_b^-},\quad G_b = \frac{\eta_b^-}{\eta_b^+} \tag{2}$$

$$\eta_i = \eta_i^+ + \eta_i^- \tag{3}$$

Here, subscripts u and b stand for unburned and burned respectively. G_u and G_b could be calculated by setting inlet and outlet boundary conditions. G_f^+ and G_f^- were functions of G_f which was the ratio of fluctuating mass flow rate for both sides of the flame. Here, G_f was designated the flame response function. Bohn and Deuker(1993) used the following simple time lag model.

$$G_f = \frac{\eta_b}{\eta_u} = \frac{1}{j\omega\tau_f}\left(1 - e^{-j\omega\tau_f}\right) \tag{4}$$

$$\tau_f = \frac{L_f}{U_f} \tag{5}$$

Here, time dependency of solution was assumed by $e^{j\omega t}$ and τ_f was lag time and passing time through the flame length. To take into account the effect of fluctuating heat release rate, Bloxidge's flame model was used.

$$q(x) = \frac{u_u}{2\pi j\omega r_B} Q(x) e^{-j\omega\tau(x)} \tag{6}$$

$$\tau(x) = x / U_f \tag{7}$$

In this model, fluctuating heat release rate was changed sinusoidally in the axial direction and it could be calculated by fluctuating inlet velocity, mean heat release rate and the passing time at the position x. To eliminate M^2 order terms, where M is Mach number, the following relation can be deduced between fluctuating inlet/outlet mass flow rate and fluctuating heat release rate.

$$\eta_b C_p T_b = \eta_u C_p T_u + \int_0^{L_f} q(x)dx \tag{8}$$

Mean heat release rate was assumed to be the following triangular distribution.

$$Q(x) = \frac{Q_m}{L_m} x \qquad (0<x<L_m) \tag{9}$$

$$Q(x) = Q_m - \frac{Q_m}{L_f - L_m}(x - L_m) \qquad (L_m<x<L_f) \tag{10}$$

The flame response function G_f was introduced from (8)-(10) by integration.

$$G_f = \frac{T_u}{T_b}\left[1 + \frac{2(T_b - T_u)}{\omega^2 \tau_m \tau' T_u}\frac{1}{j\omega\tau_f} \times \left\{\frac{L_f}{L_f - L_m} e^{-j\omega\tau_m} - \frac{L_m}{L_f - L_m} e^{-j\omega\tau_f} - 1\right\}\right] \tag{11}$$

$$\tau_m = \frac{L_m}{U_f},\ \tau' = \frac{2\pi r_B}{U_u} \tag{12}$$

Here, U_u was the velocity at the outlet of the burner. The passing time was calculated by the following formula using turbulent flame speed S_t.

$$\tau_f = \frac{L_f}{U_f} = \frac{1}{U_f}\sqrt{\frac{(r_o^2 - r_B^2)U_u \cos\vartheta}{S_t \tan\vartheta}} \qquad (13)$$

Here, U_f was not equal to U_u and assumed to be proportional to the velocity U_u because the flame was divergent radially.

$$U_f = 0.43 \times U_u \qquad (14)$$

The dependency of pressure, fuel- air-ratio, and velocity could be considered through S_t where ϑ was flame angle. Turbulent flame speed could be calculated by the author's HTA model which assumed a temperature profile across the flame was a hyperbolic tangent profile and the reaction rate was an Arrehnius type.

$$S_t = S_u(1 + (0.056R_t)^2)^{0.5} \qquad (15)$$

$$S_u = P^{-0.5}\sqrt{\frac{\lambda}{C_p}\frac{\alpha A_{O2}}{M_{O2}}\left\{Y_2\frac{1}{\chi^2}\left(\frac{T_b}{E_0}\right)^2 + Y_3\frac{1}{\chi}\left(\frac{T_u}{E_0}\right)\right\}} \exp\left(-\frac{E_0}{2T_b}\right) \qquad (16)$$

$$Y_2 = 1 - Y \qquad (17)$$

$$Y_3 = 1 - \frac{Y}{Y_{st}} \qquad (18)$$

$$\chi = \frac{(T_b - T_u)}{T_u} \qquad (19)$$

Here, R_t was the turbulent Reynolds number and calculated by turbulent velocity v_t, the Taylor microscale l_t and laminar kinematic viscosity ν.

$$R_t = \frac{v_t l_t}{\nu} \qquad (20)$$

S_t/S_u was proportional to R_t at high R_t, which was the same as the Andrews's formula (1975). The pressure dependency of R_t was mainly introduced by laminar kinematic viscosity at the condition of constant velocity. Fig.3 shows experimental results of v_t, l_t, and R_t, for cold flows in the same combustion chamber (Hayashi et al.(1995)). Flow was not the same as that of this study but the grid generated turbulence through gauze. Average axial velocity was fixed as 6m/s and a hot wire anemometer was used forturbulence measurement. Turbulent velocity increased, the Taylor microscale decreased and R_t increased with increasing pressure. The power of pressure was 0.62 for R_t between 0.4 - 10 MPa.

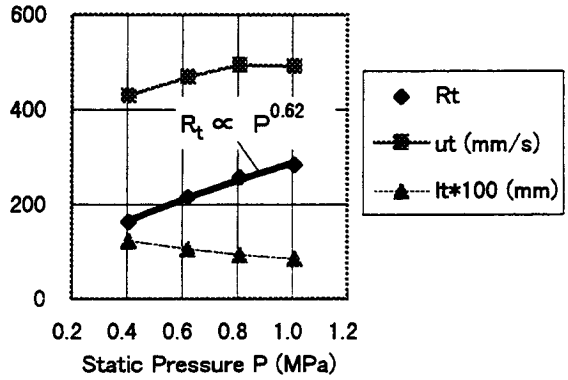

Figure 3. Turbulent Flame Speed (Hayashi et al.(1995))

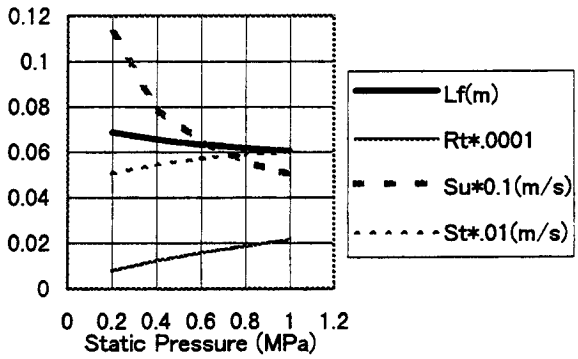

Figure 4. Pressure dependency of quantities (T_u=388°C, F/A=0.038)

The power has not been fixed and varied from 0.5 to 0.25 for various investigators(Andrews(1975), Bradley(1992)). In this study, our experimental results, which covered the pressure range of this study, was used. The correlation was set as follows.

$$R_t = \left(\frac{0.14U_u r_B}{\nu}\right)^{0.62} \qquad (21)$$

The pressure dependency of some quantities are shown in Fig.4. Laminar flame speed of methane decreased with static pressure, but turbulent Reynolds number increased with it. Turbulent flame speed increased with static pressure because turbulent Reynolds number was more sensitive and flame length decreased with static pressure. Temperature dependency was also considered for viscosity, heat conduction rate and heat capacity.

Examples of the flame response function are shown in Fig.5. The imaginary part of the response function is proportional to the oscillation energy generated at the flame. The oscillation energy generated at the flame can be calculated because of the Rayleigh's criterion and the approximation of $O(M^2)$ by the difference of

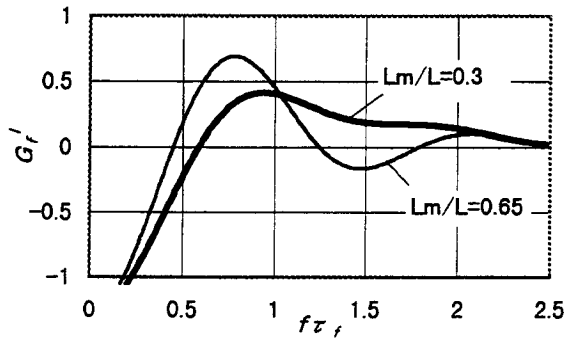

Figure 5. Flame Response Functions
(T_u=388°C, F/A=0.038)

acoustic energy between the leading and the following edges of the flame.

$$\begin{aligned}\Delta W &= W_b - W_u \\ &= \int (\dot{p}_b^R \dot{u}_b^R - \dot{p}_u^R \dot{u}_u^R) dt \\ &= (p_b^R u_b^R + p_b^I u_b^I) - (p_u^R u_u^R + p_u^I u_u^I) \end{aligned} \quad (22)$$

Here, dots indicate the quantity including $e^{j\omega t}$. In general, the absolute value of acoustic energy at leading edge is less than that at the following edge, because acoustic energy is zero in a uniform media and enthalpy fluctuation at the flame is transported downstream. Then $W_b \gg W_u$ and oscillation energy would be approximately proportional to the imaginary part of the response function as follows.

$$\Delta W \cong (p_u^I u_u^R - p_u^R u_u^I) G_f^I \quad (23)$$

The sign of the oscillation energy was changed by p_u, u_u and G_f^I and the value in parenthesis depended on the flame region in the acoustic standing wave. The parenthesis term was negative where the standing wave changed from a node to antinode axially and positive where the standing wave changed from an antinode to node axially. The response function G_f^I was varied with $f\tau_f$ and L_m/L_f as shown in Fig.5. G_f^I was changed from positive/negative to negative/positive alternately with increasing $f\tau_f$ and it diminished gradually at large $f\tau_f$ because of the trianglular distribution of heat generation rate. Combustion oscillation occurred when $f\tau_f$ satisfied the oscillation condition ΔW>0. Pressure, F/A , inlet velocity and temperature affected τ_f through inlet velocity U_u and flame length L_f which was dependent on flame speed and turbulent Reynolds number.

Fluctuating pressure mode in the acoustic system was calculated by the transfer matrix calculation including the flame. The transfer matrix of the flame was written as follows.

$$\begin{bmatrix} p_b \\ \eta_b \end{bmatrix} = \begin{bmatrix} 1 & 0 \\ 0 & G_f \end{bmatrix} \begin{bmatrix} p_u \\ \eta_u \end{bmatrix} \quad (24)$$

Here, fluctuating pressure was assumed to be unchanged on both sides, upstream and downstream.

In the analysis, the calculational domain covered the area from the baffle plate inside the premixer to the choke orifice at the outlet of the combustion chamber. The inlet boundary condition was assumed to be open ($p=0$) and the outlet condition was assumed to be closed ($\eta=0$). The flow path was divided into 8 elements including baffle plate, premixer, inlet pipe, swirl vane, ring, flame, combustion chamber and choke which were modeled by straight pipes with the same area. For each pipe, a simple transfer matrix was assumed as follows.

$$\begin{bmatrix} p_{i+1} \\ \eta_{i+1} \end{bmatrix} = \begin{bmatrix} \cos(kl) & -j\varsigma \sin(kl) \\ -j\frac{1}{\varsigma}\sin(kl) & \cos(kl) \end{bmatrix} \begin{bmatrix} p_i \\ \eta_i \end{bmatrix} \quad (25)$$

$$\varsigma = \frac{a}{S} \quad (26)$$

The attenuation was considered by using imaginary wave number. The ratio Γ of imaginary to real parts of wave number was assumed by the following expression for a smooth pipe.

$$\Gamma = -1.24 \times 10^{-5} a \sqrt{\frac{\pi}{4S\omega}} \quad (27)$$

The matrix (25) was also used to calculate acoustic impedance upstream and downstream of the flame and to calculate the acoustic amplifying factor G. The stability of combustion oscillation could be evaluated by G and eq. (22) in turn for calculating G. The oscillation energy ΔW could be calculated by the acoustic resonance mode and using eq.(22). Both methods were applied to the analysis. Here, the modes for various conditions were normalized at the outlet of the combustion chamber.

RESULTS

Fig.6 shows the time averaged light emission distribution of flame which was measured by a CCD camera from a window located at the side wall of the test section (Fig.1). Fig.6 also shows mean light emission distribution, which was calculated by light emission at the centerline, because the window couldn't cover the whole flame. Pressure was 0.63MPa, inlet temperature was 395°C, fuel-to-air ratio was 0.04 and air flow rate was 0.27kg/s.

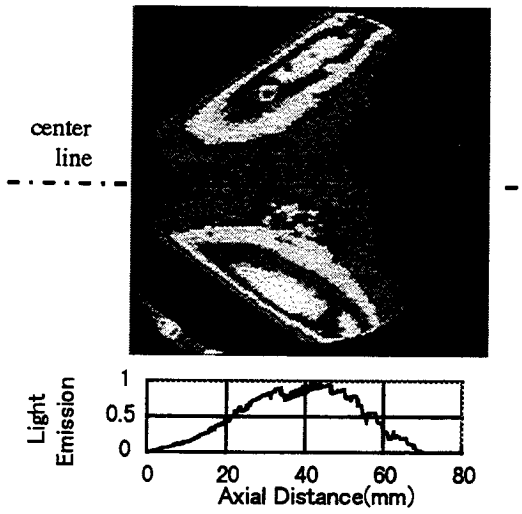

Figure 6. Mean Light Emission Distribution
(T_u=395°C, F/A=0.04, 0.63MPa)

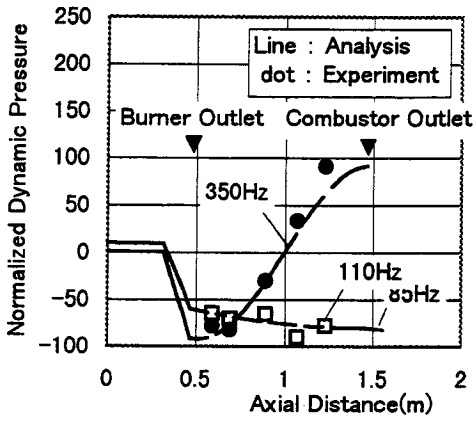

Figure 7. Fluctuating Pressure Mode
(T_u=385°C, F/A=0.04, 1.21MPa)

The flame diverged from the outlet of the burner at 30 degree which was almost the same as the swirl angle. Axial mean light emission distribution was triangular as assumed in Eqs.(9) and (10). L_m/L_f was 0.65 and the value was used in the analysis. This kind of image processing clarified that flame length was shortened with increasing pressure and that the high intensity region was transported from upstream to downstream. Such observations were important to evaluate the characteristics of combustion oscillation because the combustion time altered the ratio of combustion to acoustic times.

Fig. 7 shows experimental and analytical axial modes of fluctuating pressure. Here, Inlet temperature was 385°C, fuel-to-air ratio was 0.04 and pressure was 1.21 MPa. There were two major peaks 350Hz and 110Hz in the fluctuating pressure spectrum. The pressure mode of 350Hz has a nodal point in the combustion chamber and antinodes at both ends of the chamber. The pressure mode of 110Hz had no nodal point in the combustion chamber and had antinodes at the outlet of the chamber. The 110Hz oscillation was the Helmholtz type oscillation with a quarter wave in an acoustic system including a combustion chamber and an inlet pipe. The analysis using the transport matrix method could simulate the shapes of these modes although the lower frequency did not agree with the experimental data. Here, the analysis results were normalyzed to fit the experimental results because the transport matrix method could not calculate the absolute amplitude of fluctuating pressure.

The combustion oscillation analysis was applied to the experiment where inlet temperature was 388°C, F/A was 0.03～0.04 and pressure was 0.66 and 0.88MPa. Only the 350Hz oscillation was observed in the fluctuating pressure spectrum. Fig. 8 shows Bode's diagrams of the acoustic amplifying factor G for the simple time lag model and the present model. Here, the quantity along the ordinate was $e^{0.1\phi}$ for the phase ϕ of G. The

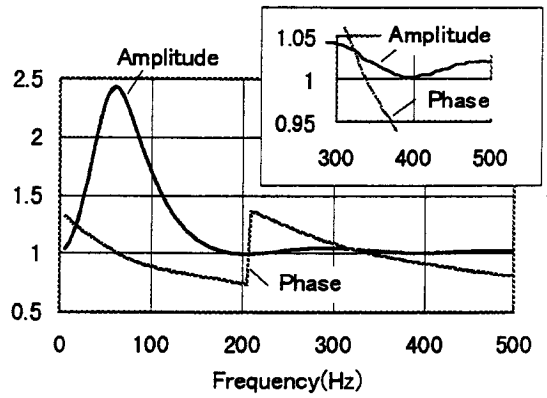

(a) Simple Time Lag Model

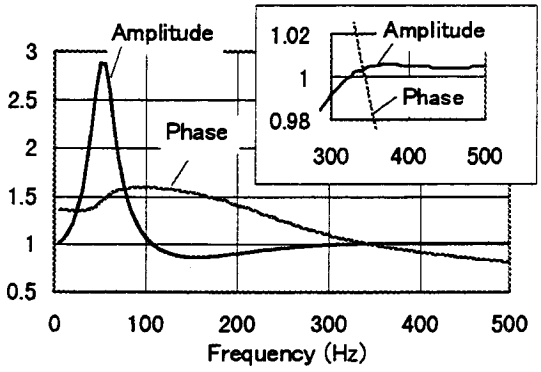

(b) Present Model
Figure 8. Bode's Diagram
(Tu=388°C, F/A=0.038, 0.66MPa)

resonance occurred where the ordinate for the phase was one. The 80Hz and 350Hz resonances were generated by the simple time lag model but the 80Hz resonance was dominant. The results was inconsistent with the experimental results. By using the present model, on the other hand, the phase ϕ was not zero at 80Hz and the resonance was suppressed. The peak which appeared around 350Hz was dominant.

Fig. 9 shows the imaginary part of the response functions of flame G_f^I. The G_f^I of the simple time lag model was always negative and, for the resonant frequency, the amplitude of G_f^I of 80Hz was larger than that of 350Hz. The 80Hz oscillation was dominant. For the present model, there was a single resonant frequency as shown in Fig. 8 and the amplitude of G_f^I had its local maximum around the 350Hz resonant frequency.

Dynamic pressure at resonant frequency which was obtained by experiment is shown in Fig.10. The ordinate is the ratio of dynamic pressure and static pressure. Dynamic pressure had its peak at specified F/A and the peak moved from large F/A to small F/A with higher pressure. Analytical results of the acoustic amplifying factor using the present model are shown in Fig.11. Here, the ordinate is the excess of the absolute value of G from one and it indicated the instability of small F/A with higher pressure. That was consistent with experimental data. The absolute value along the ordinate could not be compared between analysis and experiment because a linear analysis was employed in this calculation. However, the pressure and the fuel-to-air ratio dependency of analysis agreed with experimental data. Following the discussion in Figs.5 and 9, combustion oscillation occurred at specified $f\tau_f$. As shown in Fig.4, turbulent flame speed increased with pressure and flame length decreased with pressure. Therefore, the resonance occurred at low F/A with increasing high pressure because flame length was kept constant with the same velocity.

Fig.12 shows the oscillation energy calculated by eq.(22) using the transfer matrix of flame. Fig.12 was almost the same as Fig.11. The 80Hz oscillation was not appeared also in this calculation. The acoustic stability could be evaluated by the simple transport matrix method using the flame matrix and without using the acoustic amplifying factor. The method using the flame transport matrix was flexible and applicable to complex geometry

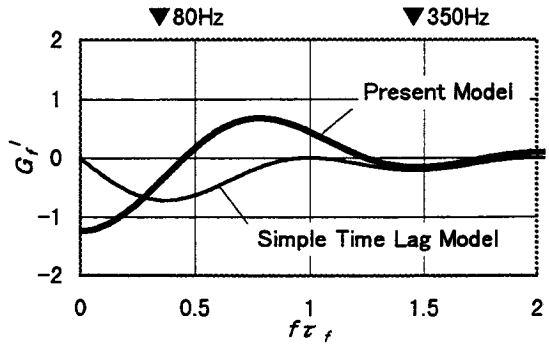

Figure9. Flame Response Function
(Tu=388°C, F/A=0.038, 0.66MPa)

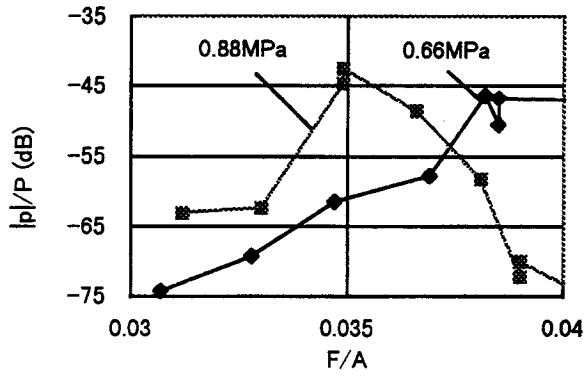

Figure 10. F/A Dependency of Dynamic Pressure (Experiment)

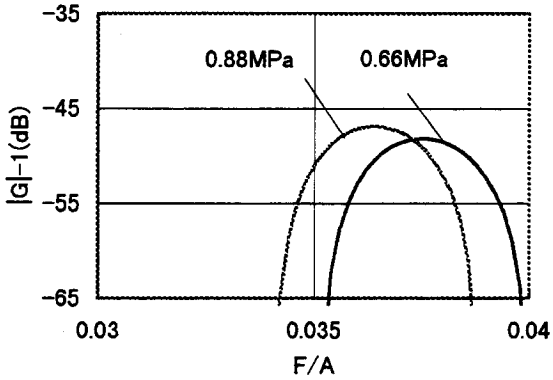

Figure 11. F/A Dependency of Dynamic Pressure (Acoustic Amplifying Factor Analysis)

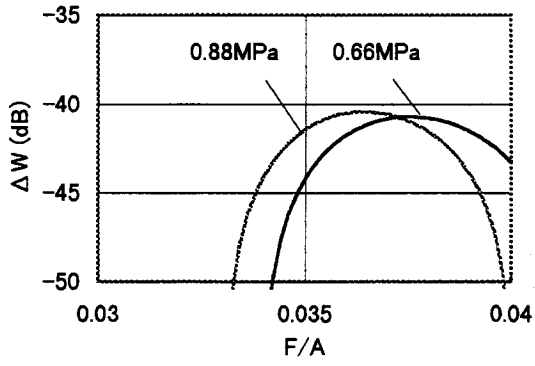

Figure12. F/A Dependency of Dynamic Pressure (Flame Matrix Analysis)

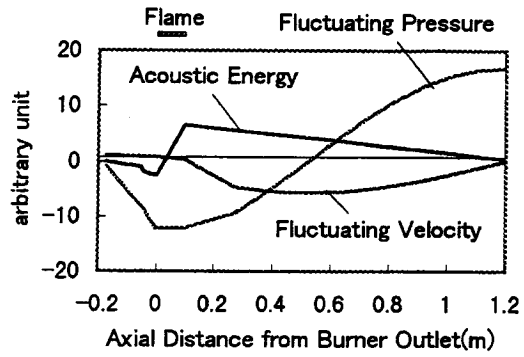

Figure 13. 350Hz Acoustic Mode
(Tu=388°C, F/A=0.038, 0.66MPa)

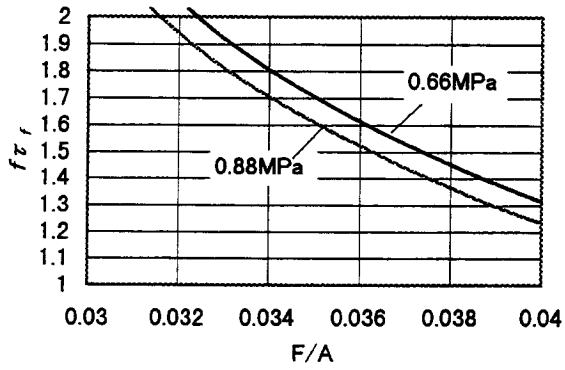

Figure 14. Pressure Dependency of $f\tau_f$

including junctions of flow paths which often appear in real configurations of commercial combustors.

Fig.13 shows the 350Hz oscillation mode calculated by the transfer matrix method using flame transfer matrix of the present model. The fluctuating pressure mode had antinodes both at the inlet and outlet of the combustion chamber and the fluctuating velocity mode had a node at the outlet of the burner. Acoustic energy W changed from negative to positive through the flame axially and oscillation energy ΔW was transferred from thermal hydraulic energy to acoustic energy. Oscillation energy generated at the flame was transported from upstream to downstream. The dissipation of acoustic energy was balanced with the energy loss along the combustion chamber wall. The positive going traveling wave was larger than the negative going traveling wave in the combustion chamber because acoustic energy vanished for the standing wave in uniform media.

Fig.14 shows $f\tau_f$ calculated by the analysis. Combustion oscillation occurred when $f\tau_f$ was equal to 1.5 where the G_f^I had its local maximum in Figs.5 and 9. As mentioned above, combustion oscillation for an almost completely premixed flame could be predicted by calculating acoustic resonance mode, the response function and $f\tau_f$.

CONCLUSION

A new analytical time lag flame model based on Bloxidge's flame model was introduced for calculating combustion oscillation of premixed flame to take into account the distribution of heat release rate and flame speed which was calculated by analytical formulas dependent on pressure, temperature, fuel-to-air ratio and velocity. Here, time lag τ_f could be calculated by analytical formulas with the authors' HTA (Hyperbolic Tangent Approximation) model. To verify the model, combustion oscillation experiments were performed for methane-air premixed flames stabilized by a swirl burner at elevated pressures between 0.6 - 0.9MPa.

The simple time lag model could not calculate the dominant frequency of oscillation. The new model, however, could simulate the pressure and F/A dependency of the maximum dynamic pressure peak.

The fluctuating pressure had its maximum peak at the specific value of $f\tau_f$ where f is the frequency of resonance. The combustion oscillation for almost completely premixed flame, therefore, could be predicted by calculating the acoustic resonance mode, the response function and $f\tau_f$.

REFERENCES

G. E. Andrews, D. Bradley and S. B. Lwakabamba, Turbulence and Turbulent Flame Propagation - A Critical Appraisal, Combust. Flame (1975) Vol.24, No. 3, p.285-304

D. Bohn and E. Deuker, An Acoustic Model to Predict Combustion driven Oscillations, 20th International Congress on Combustion Engines, G20, London, 1993

G.J. Bloxidge, A.P. Dowling and P.J. Langhorn, Reheat Buzz : An Acoustically Coupled Combustion Instability, J. Fluid Mech. (1988) Vol.193, pp.445-473

D. Bradley, How Fast can we burn?, 24th Int. Symp. on Combust., (1992) Sydney

S. Candel, C. Hyunh and T. Poinsot, Some Modeling Methods of Combustion Instabilities, C0593B NATO ASI Ser. E (1996) Vol.306,, pp.83-112

A. Hayashi, S. Inage, S. Dodo, K. Ito, M. Ohtsuka and S. Tonosu, Evaluation of the Effect of Pressure on Turbulent Burning Velocity, Proc. of JSME FED Conf. (199ν5), in Japanese

S. Inage and M. Ohtsuka, A Proposal for a New Turbulent Premixed Combustion Model and Its Evaluation (Development of the Model), JSME Int. J (1996) Series B, Vol.39, No.3, pp.640-646

R. J. Raun, M. W. Beckstead, J. C. Finlinson and K. P. Brooks, A Review of Rijke Tubes, Rijke Burners and Related Devices, Prog. Energy Combust. Sci. (1993) Vol.19, pp.313-364